NASA TM-87701

NASA Technical Memorandum 87701

NASA-TM-87701 19860014384

A SPECTRAL MULTI-DOMAIN TECHNIQUE WITH APPLICATION TO GENERALIZED CURVILINEAR COORDINATES

MICHÈLE G. MACARAEG AND
CRAIG L. STREETT

Corrected Copy

MARCH 1986

LIBRARY COPY

MAY 14 1986

LANGLEY RESEARCH CENTER
LIBRARY, NASA
HAMPTON, VIRGINIA

NASA
National Aeronautics and
Space Administration

Langley Research Center
Hampton, Virginia 23665

A Spectral Multi-Domain Technique With Application to Generalized Coordinates

Michèle G. Macaraeg and Craig L. Streett
NASA Langley Research Center

INTRODUCTION

Spectral collocation methods have proven to be efficient discretization schemes for many aerodynamic (see e.g., refs. 1-5) and fluid mechanic (e.g., refs. 6-9) problems. The high-order accuracy and resolution shown by these methods allows one to obtain engineering-accuracy solutions on coarse meshes, or alternatively, to obtain solutions with very small error. One drawback to these techniques has been the requirement that a complicated physical domain must map onto a simple computational domain for discretization. This mapping must be smooth if the high-order accuracy and exponential convergence rates associated with spectral methods are to be preserved (ref. 2). Additionally even smooth stretching transformations can decrease the accuracy of a spectral method, if the stretching is severe (ref. 5). A further difficulty with spectral methods has been in their implementation on parallel processing computers, where efficient spectral algorithms have been lacking.

The above restrictions are overcome in the present method by splitting the domain into regions, each of which preserve the advantages of spectral collocation, and allow the ratio of the mesh spacings between regions to be several orders of magnitude higher than allowable in a single domain. Such stretchings would be required to resolve the thin viscous region in an external aerodynamic problem. Adjoining regions are interfaced by enforcing a global flux balance which preserves high-order continuity of the solution, regardless of the type (diffusion- or advection-dominated) of the equations being solved. This interface technique maintains spectral accuracy, even when mappings and/or domain sizes are radically different across the interface, provided that the discretization in each individual subdomain adequately resolve the solution there. Additionally, the present technique allows spectral collocation methods to efficiently utilize parallel processing (ref. 10) where the application of conventional single-domain spectral discretizations have not been found to be efficient.

A number of other spectral multi-domain techniques have appeared in the literature. Application of finite element methodology, using Galerkin spectral discretization in the variational formulation within the elements, is a popular

N86-23855#

technique (refs. 11-12). One drawback with such techniques is that a split Galerkin-collocation discretization must be used for convection-diffusion problems. These spectral-element methods also seem to work best in practice when used in a manner similar to classical finite element techniques: low-order internal discretization using many elements with no internal stretchings to improve resolution. In other words, resolution is increased in such methods by packing more elements in appropriate areas, rather than by increasing the order of discretization or applying an appropriate stretching within an element. The use of low-order spectral discretization over many elements does not take advantage of the exponential order convergence properties of spectral methods even if the split Galerkin-collocation discretization can display such properties. Techniques which the authors are aware of for interfacing collocation-discretized domains seem to involve explicit enforcement of continuity of the solution and its first derivative across the interface (refs. 13-14). It is not clear how well these techniques perform for strongly convection-dominated problems; the second author's experience with such techniques (ref. 1) has shown them to be not entirely satisfactory.

Results

In this section, the present global flux-balance spectral multi-domain method will be shown as applied to a number of one- and two-dimensional test problems. (Detailed explanation concerning the implementation of the algorithm is given in ref. 10.) The one-dimensional examples will serve to show that this method can maintain the exponential-order error convergence which is characteristic of collocation methods, even when adjoining domains have radically different discretizations in terms of domain size, number of points, or stretchings.

The first example is the equation

$$U_{xx} = \cos\ \frac{\pi x}{4};\ x\varepsilon[-2,2], \quad U(-2) = U(2) = 0 \tag{1}$$

for which the exact solution is:

$$U(x) = \frac{-16}{\pi^2}\ \cos\frac{(\pi x)}{4} \tag{2}$$

Eq. (1) is discretized in two unstretched domains: $x^{(1)}\varepsilon$ [-2,0]; $x^{(2)}\varepsilon$ [0,2], with N1 and N2 points, respectively. In table I is listed the maximum relative error as a function of N1 and N2. Note that the error decay is clearly faster than algebraic down to machine zero when N1 = N2. Also shown in table I is the behavior of the solution when one discretization is held fixed (N1) and the other refined (N2). The overall error remains constant at a level essentially one-half of that seen when both domains were discretized at the coarser level. This is expected behavior, since the error in the interface condition has components from both domains; if one discretization is very much coarser than the other, its error will dominate the overall error of the solution. When both have equal error, then they must contribute equally to the overall error.

The next example will illustrate the capability of the method for resolving very high gradients in a solution while imposing an interface condition which preserves spectral accuracy. Consider the viscous Burger's equation:

$$U_t + \frac{1}{2}\,(U^2)_x = \nu\, U_{xx};\ x\ \varepsilon\ [-1,1] \tag{3}$$

$$U(-1,t) = U(1,t) = 0 \qquad U(x,0) = -\sin(\pi x)$$

This problem has been studied extensively by a number of authors, using techniques ranging from standard finite difference, to single-domain spectral collocation and spectral element (ref. 15). The solution to this problem develops a very steep gradient region in the center of the domain; the slope at x = 0 reaches a maximum, then decreases as the initial energy is dissipated away. For the parameters studied in ref. 15 ($\nu = 0.01/\pi$), this maximum is reached at t = 0.5; a very accurate analytical solution gives a value of 152.00516 for this

maximum slope. The evolution of this solution calculated from the present method is shown in fig. 1 at time increments of 0.1.

In the present study of this problem, three domains were used, the middle domain spanning a very small region (±0.05) around the "shock." Additionally, a mapping was applied in the middle domain to improve resolution. The maximum stretching allowable in this mapping is subject to the same restriction as stretchings in single-domain discretizations; e.g., maximum metric ratios on the order of 10^3.

From the comparison study contained in ref. 15 the two methods giving the best accuracy for a given number of grid points were single domain spectral collocation and spectral element. The collocation scheme used a mesh stretching with a maximum-to-minimum metric ratio of about 100. Beyond this stretching a degradation in accuracy was found to occur. The spectral element discretization utilized four elements with 16 nodes in each. The behavior of the error in maximum slope from these methods and the present scheme are shown in table II. As can be seen, the present method with just 35 total points (12 points in the outer domain, 13 points in the middle domain, 12 points in the left outer domain, hereafter denoted 12/13/12) yield results of equivalent accuracy to the spectral element and single-domain spectral collocation methods of ref. 16 both using 64 total points. Further mesh refinements using the present method show exponential-order error convergence, as seen in table II by the order-of-magnitude decrease in relative error as the mesh is refined to 20/21/20, and again with mesh refinement to 32/33/32. For the same total number of points, the present method is an order of magnitude more accurate than the single-domain collocation or spectral element solutions of ref. 15.

In order to demonstrate the capability of the present method to handle radically-different mappings between adjacent domains, a solution to the above viscous Burger's equation for $\nu = 10^{-4}$, is shown in fig. 2. The maximum slope for this solution is greater than 5000. The discretization used was 12/31/12; the stretching in the middle domain was so severe that the ratio of largest mesh spacing in the outer domains to the smallest in the middle domain is greater than 10^5. A factor of 5000 magnification of the high-gradient region of this solution is shown in fig. 3. The emphasis in this plot is the oscillation-free resolution of this region. (Linear interpolation between points is used for plotting, making the plot appear somewhat jagged.)

To demonstrate the maintenance of conservation by the present interface technique, an initial condition was applied to the viscous Burger's equation to generate a moving "shock" which passed through the interface, as shown in fig. 4. No oscillations, reflections, or abrupt changes in wave speed are seen as the "shock" passes through the interface. A very skewed discretization of 12/17/27 was used for this case. Note that a multi-domain method formulated only for hyperbolic or for elliptic equations would be unable to perform well on this problem, since the dissipation-dominated region passes through the interface.

Two-dimensional examples show similar performance of the present method. Shown in fig. 5 are constant-value contours for the solution of the Poisson equation:

$$U_{xx} + U_{yy} = \cos\frac{(\pi y)}{2} \cdot \cos\frac{(\pi x)}{4}; \; x \in [-2,2], \; y \in [-1,1] \qquad (4)$$

$$U(x,-1) = U(x,1) = U(-2,y) = U(2,y) = 0$$

using two domains interfaced at $x = 0$ (the dashed line in fig. 5). Note that the contours pass smoothly through the interface.

Table III contains the maximum relative error for various multi-domain discretizations of eq. (4). Exponential-order error convergence is again apparent from the rapid decrease with mesh refinements. The first group of results in table III is for equal discretization in both domains, whereas the

second group shows the effect of having different discretizations in the direction along the interface. Only a small amount of accuracy is lost through the interpolation between two radically-different discretizations across the interface.

An example of discretization on four domains with a corner point is shown in fig. 6, where isolines of the spectral solution to

$$\nabla^2 U = \cos\left(\frac{\pi x}{4}\right) \cdot \cos\left(\frac{\pi y}{4}\right), \quad x \in [-2,2],\ y \in [-2,2] \qquad (5)$$

$$U(x,-2) = U(x,2) = U(-2,y) = U(2,y) = 0$$

are displayed. An influence-coefficient matrix algorithm described in ref. 10 was used to compute this solution. This algorithm was developed for parallel-processor applications.

Spectral discretization of problems with discontinuous coefficients or source terms (or equivalently, discontinuous transformation metrics), or discontinuities in boundary condition typically yields solutions with large oscillations and low-order error convergence. The present multi-domain technique may be used to isolate such discontinuities and recover exponential-order convergence. Figs. 7 and 8 illustrate such an application; shown are solutions to Laplace's equation in which a jump in boundary conditions is enforced on one side of the domain. When the discontinuity lies at a point interior to one of the discretizations (fig. 7), oscillations are seen clearly in the solution isolines. When the discontinuity occurs where the interface meets the boundary, however, the contour lines are smooth (fig. 8).

Another example of the application of the multi-domain technique to isolate a discontinuity is in solution of the following equation:

$$\nabla \cdot (k \nabla U) = 0; \quad x \in [-2,2],\ y \in [-1,1] \qquad (6)$$

$$U(x,-1) = U(x,1) = U(-2,y) = 0 \qquad U(2,y) = \cos\left(\frac{\pi y}{2}\right)$$

where $k = k_1$, $-2 \leq x \leq 0$, and $k = k_2 = 10\, k_1$, $0 < x \leq 2$, with the interface at the line of coefficient discontinuity as shown in fig. 9. The computed solution is everywhere smooth, and the gradient jump at $x = 0$ is automatically enforced.

To demonstrate the generality of the technique, eq. (4) was solved on the skewed two-domain mesh shown in fig. 10. This mesh, containing 17 x 16 and 18 x 17 points in the left and right domains, respectively, was generated by first choosing the interface line, in this case a cubic polynomial. Chebyshev distributions with respect to arc length were used to establish the mesh points on the interface, as well as along the domain boundaries at $x = \pm 2$. One curvilinear coordinate family was generated by connecting these corresponding points with straight lines. Mesh points along these coordinate lines were then established with Chebyshev distributions with respect to arc length, resulting in a sheared non-orthogonal mesh. Eq. (4) was written in generalized contravariant flux form; the metrics were evaluated by spectral differentiation of the coordinate distributions. The flux component normal to the interface was taken to be continuous in the interface condition. As can be seen in the isolines of the solution shown in fig. 11, the solution is everywhere smooth and regular.

Conclusions

The present global flux balance spectral multi-domain method has demonstrated maintenance of exponential-order accuracy herein on a variety of advection- and diffusion-dominated test problems. Extremely large difference in discretization across an interface, through domain size, number of points and stretchings, have been shown to not disrupt this property of the present method. Additionally, this technique can be used to isolate certain types of coefficient, mapping or

boundary condition discontinuities. A further application of the present method lies in implementation of spectral methods on parallel-processing computers, where the global nature of collocation methods have limited their effectiveness. The solution algorithm described is well-suited for machines with only nearest-neighbor connections between processing units.

Further areas of applications being examined for the present method include implementation (1) in a time-dependent incompressible Navier-Stokes code for transition simulation, which will be run on the large scale Navier-Stokes Computer parallel computer under construction at Princeton University (private communication with D. Nosenchuck, Princeton University), and (2) in an external-aerodynamic compressible Navier-Stokes scheme which will interface a fine discretization of a nearfield region and a coarse discretization of the farfield to reduce storage and increase convergence rate.

References

1 Gottlieb, D. L.; Lustman, L.; and C. L. Streett: Spectral Methods for Two-Dimensional Shocks. ICASE Report No. 82-83, Nov. 1982.

2 Streett, C. L.: Spectral Method for the Solution of Transonic Potential Flow About an Arbitrary Two-Dimensional Airfoil. AIAA Paper No. 83-1949-CP. Paper presented at the AIAA 16th Computational Fluid Dynamics Conference, Danvers, MA, July 13-15, 1983.

3 Hussaini, M. Y.; Streett, C. L. and Zang, T.: Spectral Methods for Partial Differential Equations. NASA CR-172248, August 1983

4 Streett, C. L.; Zang, T. A.; and Hussaini, M. Y.: Spectral Multigrid Methods with Appliations to Transonic Potential Flow. Journal of Computational Physics, Vol. 56, 1984.

5 Streett, C. L.; Zang, T. A.; and Hussaini, M. Y.: Spectral Methods for Solution of the Boundary-Layer Equation. AIAA Paper 84-0170. Paper presented at the AIAA 22nd Aerospace Sciences Meeting, Reno, NV, Jan. 9-12, 1984.

6 Macaraeg, M. G.: Numerical Experiments of Axisymmetric Flow in a Nonuniform Gravitational Field, AIAA Journal, July 1986.

7 Macaraeg, M. G.: The Effect of Power Law Body Forces on a Thermally-Driven Fluid Between Concentric Rotating Spheres. Journal of the Atmospheric Sciences, Vol. 43, Feb. 1986.

8 Macaraeg, M. G.: A Mixed Pseudospectral/Finite Difference Method for the Axisymmetric Flow in a Heated, Rotating Spherical Shell. Journal of Comutational Physics, Vol. 61, 1985.

9 Malik, M. R.; Zang, T. A.; and Hussaini, M.: A Spectral Collocation Method for the Navier-Stokes Equations. NASA CR-172365, June 1984.

10 Macaraeg, M. G.; Streett, C. L.: Improvements in Spectral Collocation Through a Multiple Domain Technique. Applied Numerical Mathematics, 1986.

11 Patera, A. T.: A Spectral Element Method for Fluid Dynamics: Laminar Flow in a Channel Expansion. Journal of Computational Physics, Vol. 54, 1984.

12 Ghaddar, N.; Patera, A. T.; and Mikic, B.: Heat Transfer Enhancement in Oscillatory Flow in a Grooved Channel. AIAA Paper 84-0495. Paper presented at the AIAA 22nd Aerospace Sciences Meeting, Reno, NV, Jan. 9-12, 1984.

13 Metivet, B.; and Morchoisne, Y.: Multi-Domain Spectral Techniques for Viscous Flow Calculations. Proceedings of the 4th Conference on Numerical Methods in Fluid Dynamics, Oct. 1981.

14 Migliore, H. H.; and McReynolds, E. G.: Multi-Element Collocation Solution for Convective Dominated Transport. Numerical Methods in Laminar and Turbulent Flow. C. Taylor, J. Johnson, and W. Smith, eds., 1983.

15 Basdevant, C.; Deville, M.; Haldenwang, P.; Lacroix, J.; Orlandi, D.; Quazzani, J.; Patera, A.; and Petret, R.: Spectral and Finite Difference Solutions of the Burgers' Equation. Computers and Fluids, Vol. 14, 1986, pp. 23-41.

Table I.- Maximum relative error vs. domain discretization for equation (1). Numerials in parentheses are powers of ten.

N_1, N_2	$\left\| \frac{u - u_{exact}}{u_{exact}} \right\|_\infty$
5, 5	1.78 (-3)
7, 7	9.81 (-5)
9, 9	2.79 (-8)
11,11	4.85 (-11)
13,13	2.10 (-13)
5, 7	8.82 (-4)
5, 9	8.88 (-4)
5,11	8.88 (-4)
7, 9	4.89 (-5)
7,11	4.90 (-5)
7,13	4.90 (-5)
9,11	1.39 (-8)
9,13	1.39 (-8)

Table II.- Maximum slope and percent relative error in maximum slope for viscous Burgers' equation (eq. (3)); comparison of present method with results from reference 15 .

Method	Discretization	Max. slope	% Relative error
Present	3 domains: 12/13/12	152.03544	1.99 (-2)
Present	20/21/20	152.00011	3.23 (-3)
Present	32/33/32	152.00513	2.14 (-4)
Spectral element (ref. 15)	4 elements: 16/16/16/16	152.04	2.29 (-2)
Spectral colloc. (ref. 15)	1 domain: 64	152.025	1.31 (-2)
exact (ref. 15)		152.00516	

Table III.- Maximum error vs. domain discretization for equation (4) .

$(N_{x1}, N_{y1}), (N_{x2}, N_{y2})$	$\left\| \frac{u - u_{exact}}{u_{exact}} \right\|_\infty$
(6, 6), (6, 6)	0.16809 (-3)
(8, 8), (8, 8)	.13260 (-5)
(10,10), (10,10)	.71081 (-8)
(12,12), (12,12)	.27290 (-10)
(16,16), (16,16)	.71054 (-13)
(6, 6), (6,12)	.44939 (-3)
(8, 8), (8,16)	.54130 (-5)
(10,10), (10,20)	.33158 (-7)

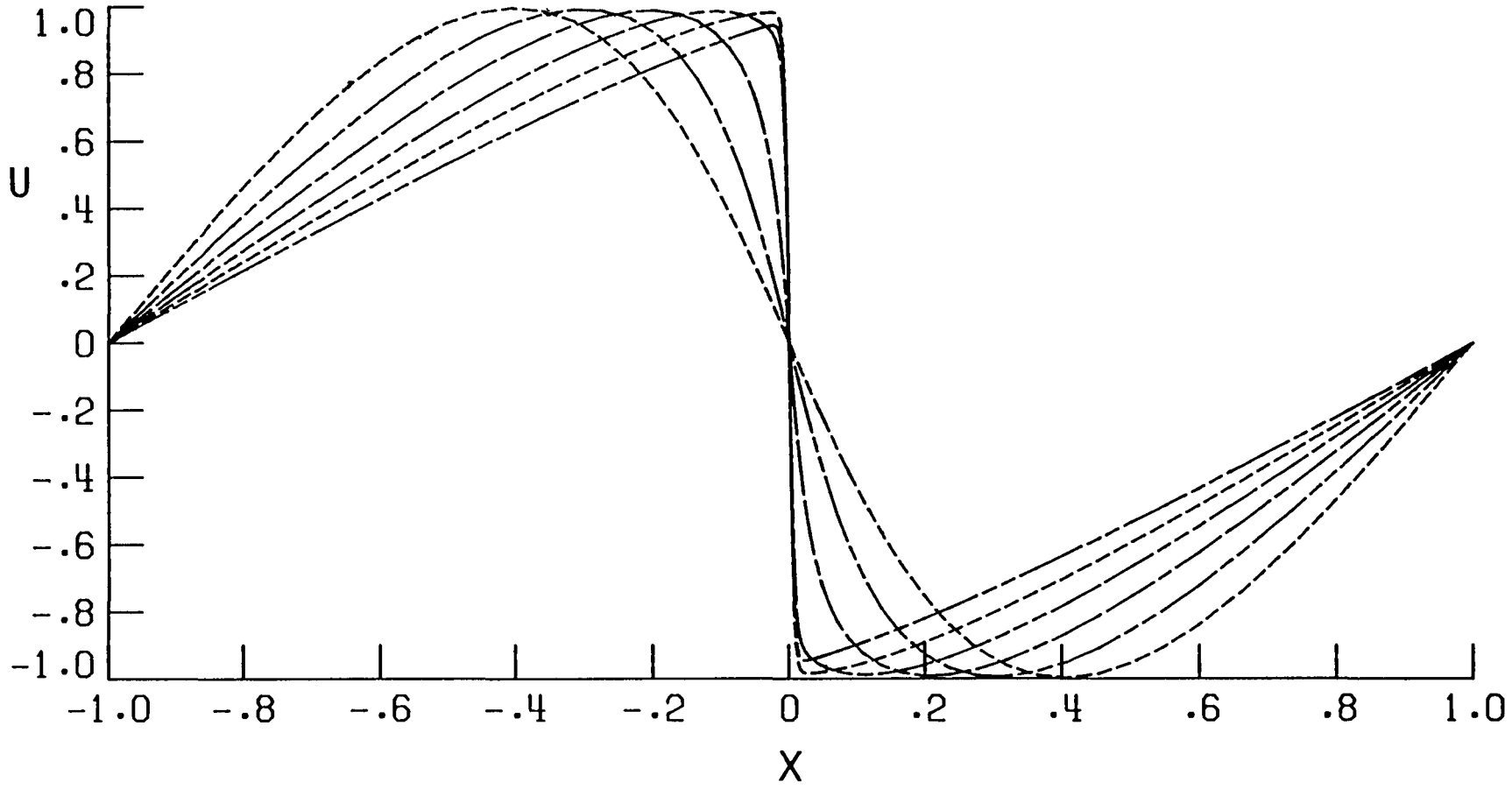

Figure 1. - Computed solution to equation (3) at time increments of 0.1: $\nu = 0.01/\pi$, discretization 32/33/32, interfaces at $\pm$ 0.05.

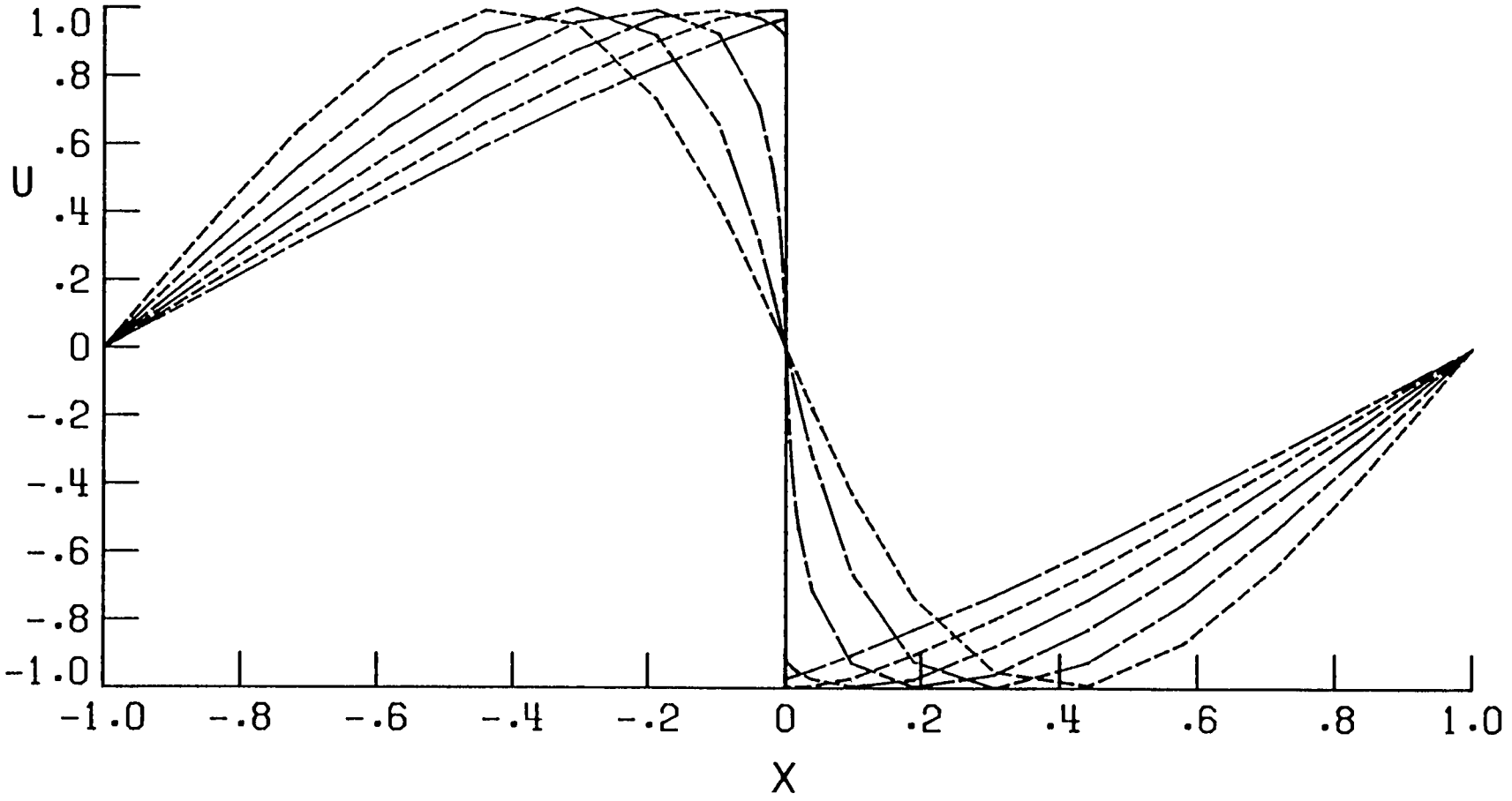

Figure 2. - Computed solution to equation (3) at time increments of 0.1: $\nu = 10^{-4}$, discretization 12/31/12, interfaces at $\pm$ 0.02.

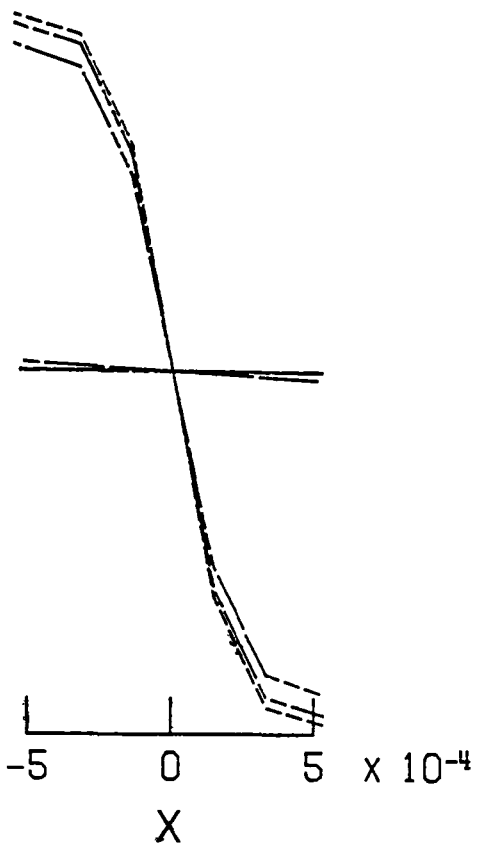

Figure 3. - Expansion of high gradient region of figure 2.

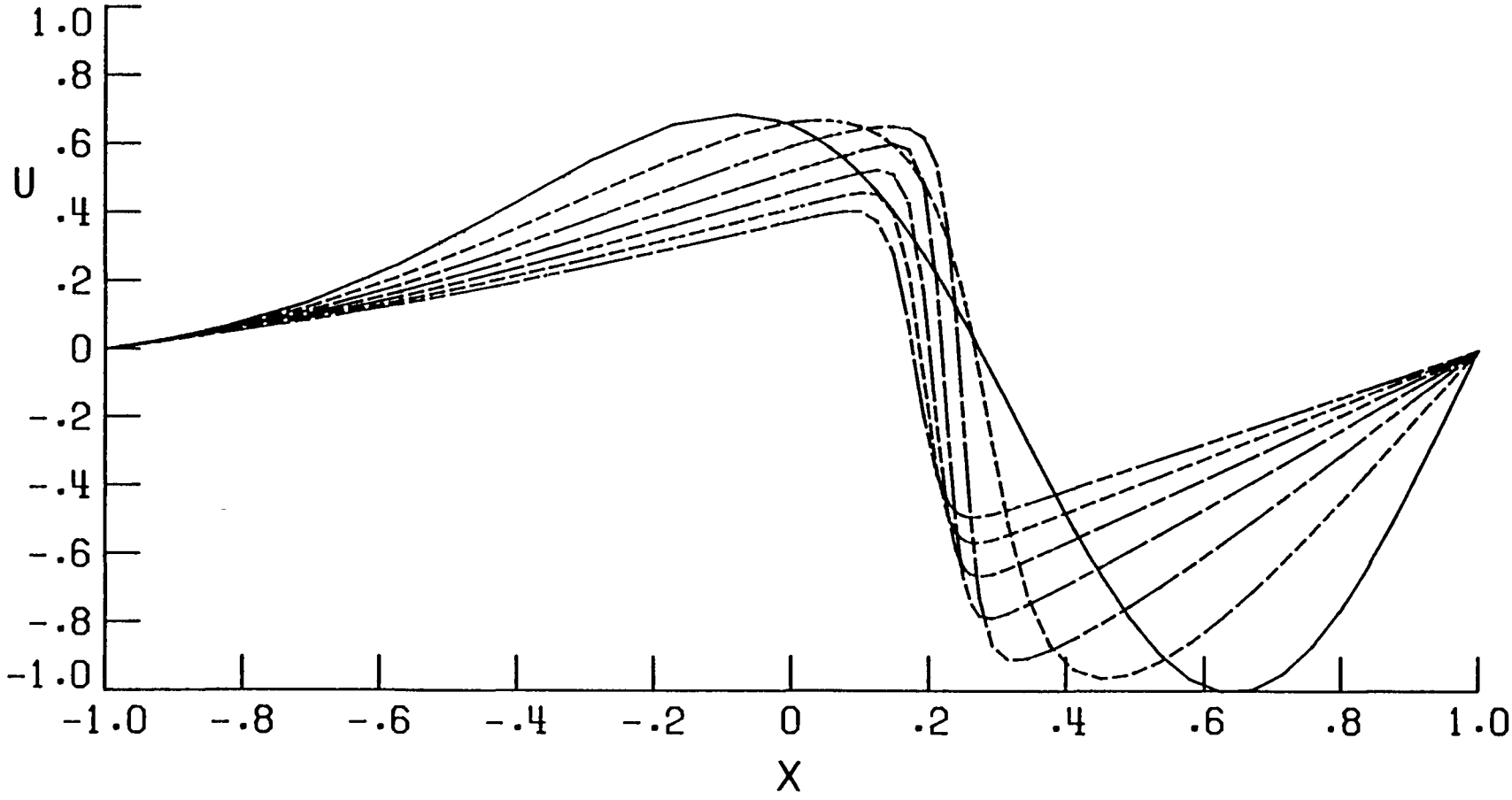

Figure 4. - Computed solution to equation (3) with moving shock: $\nu = 0.01$, discretization 12/17/27, interfaces at $\pm$ 0.25.

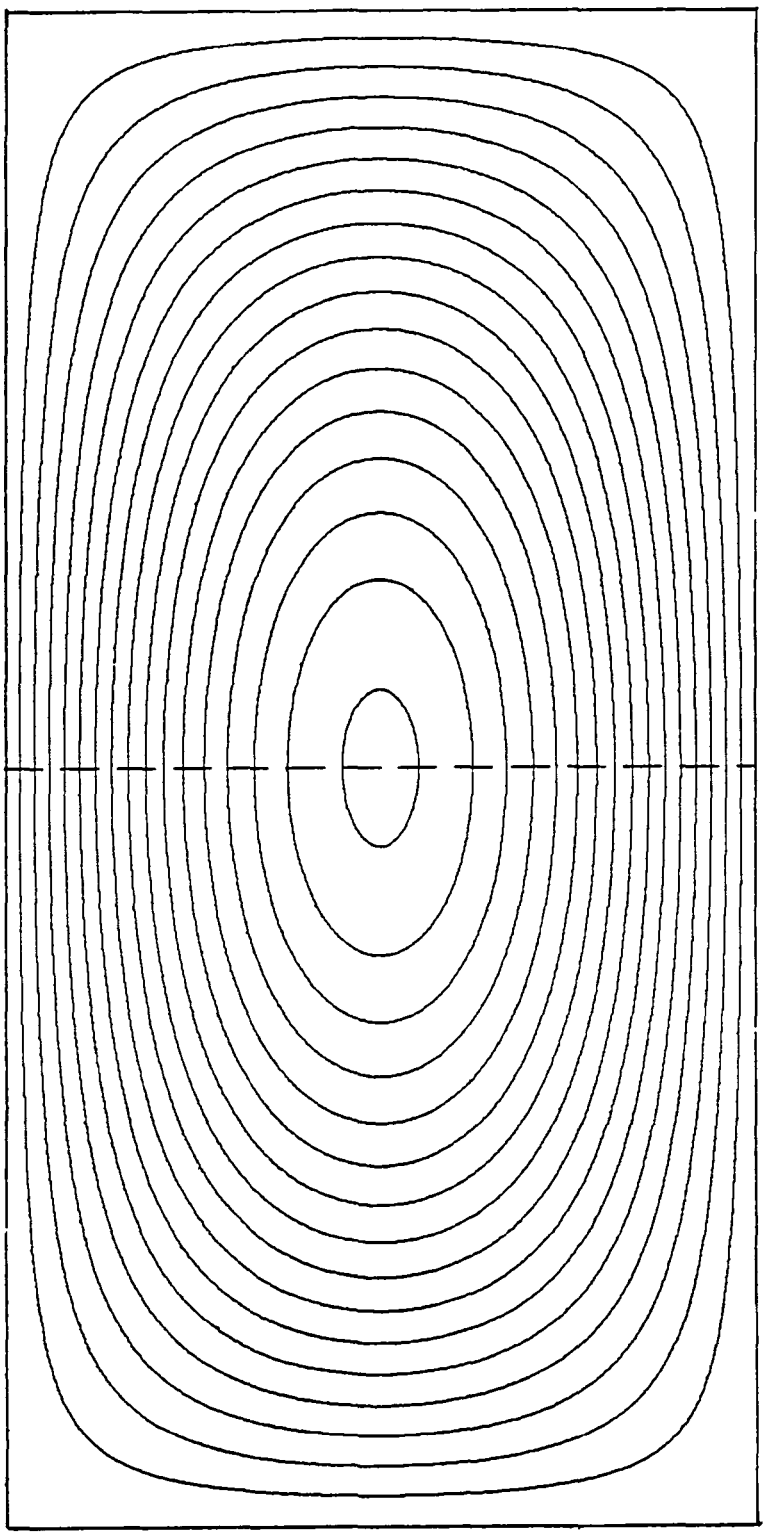

Figure 5. - Computed solution to equation (4); interface at dotted line.

Solution of Poisson eqn on Four Domains

$$u_{xx} + u_{yy} = \cos(\pi x/4)\cdot\cos(\pi y/4)$$

D: $x\epsilon[-2,2]$, $y\epsilon[-2,2]$, $u=0$ on ∂D

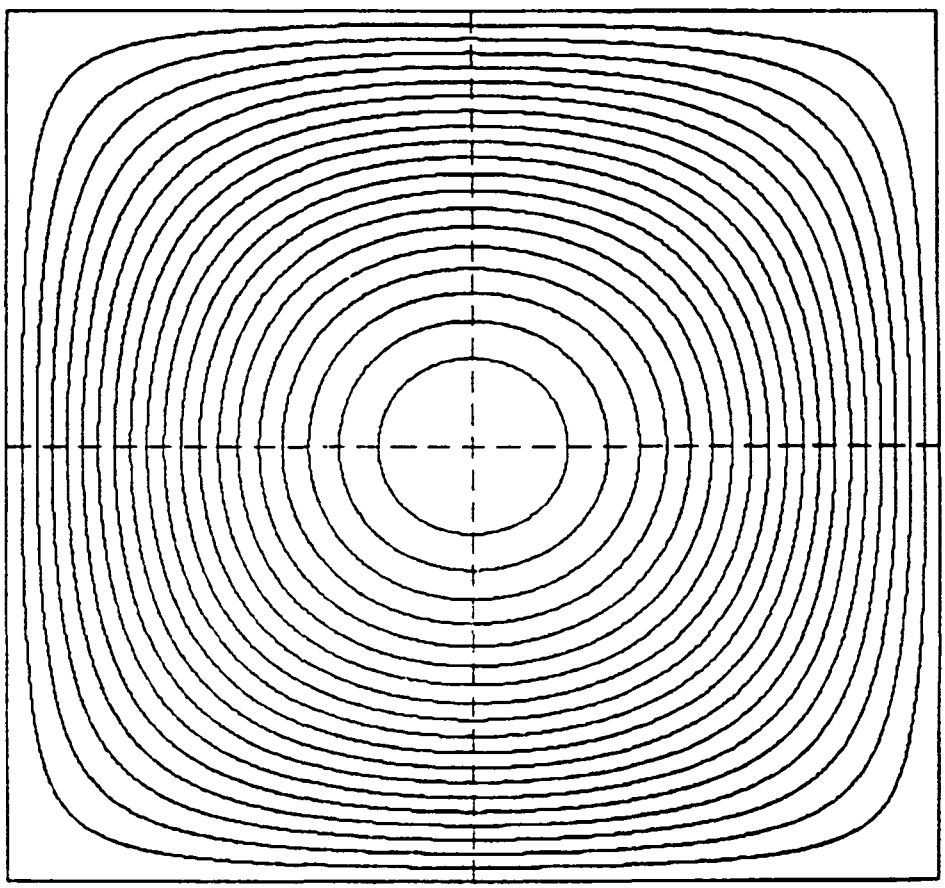

Figure 6. - Computed solution to equation (5) on four domains; interfaces at dotted lines.

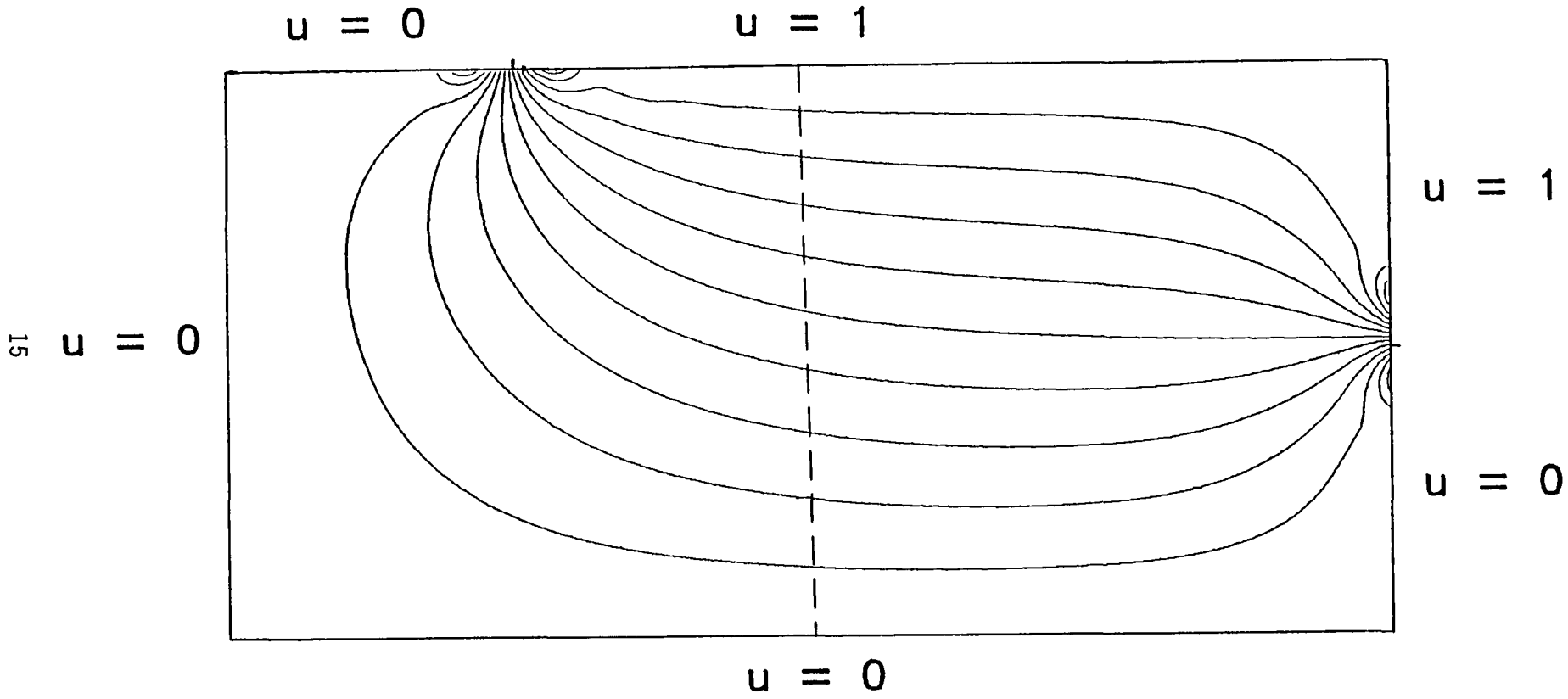

Figure 7. - Computed solution to Laplace's equation with discontinuous boundary conditions as noted; interface at dotted line.

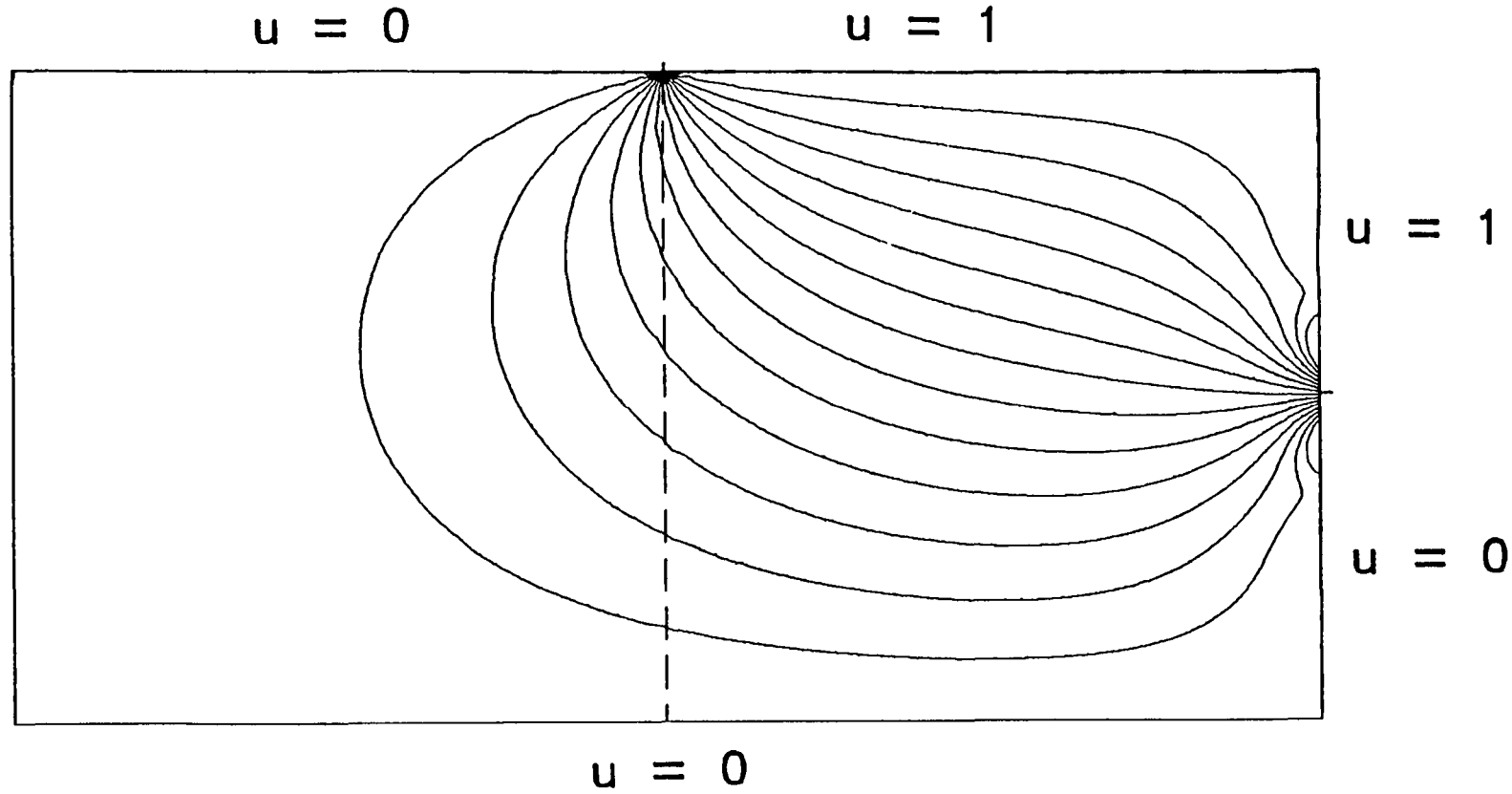

Figure 8. - Computed solution to Laplace's equation with discontinuous boundary conditions as noted; interface at dotted line.

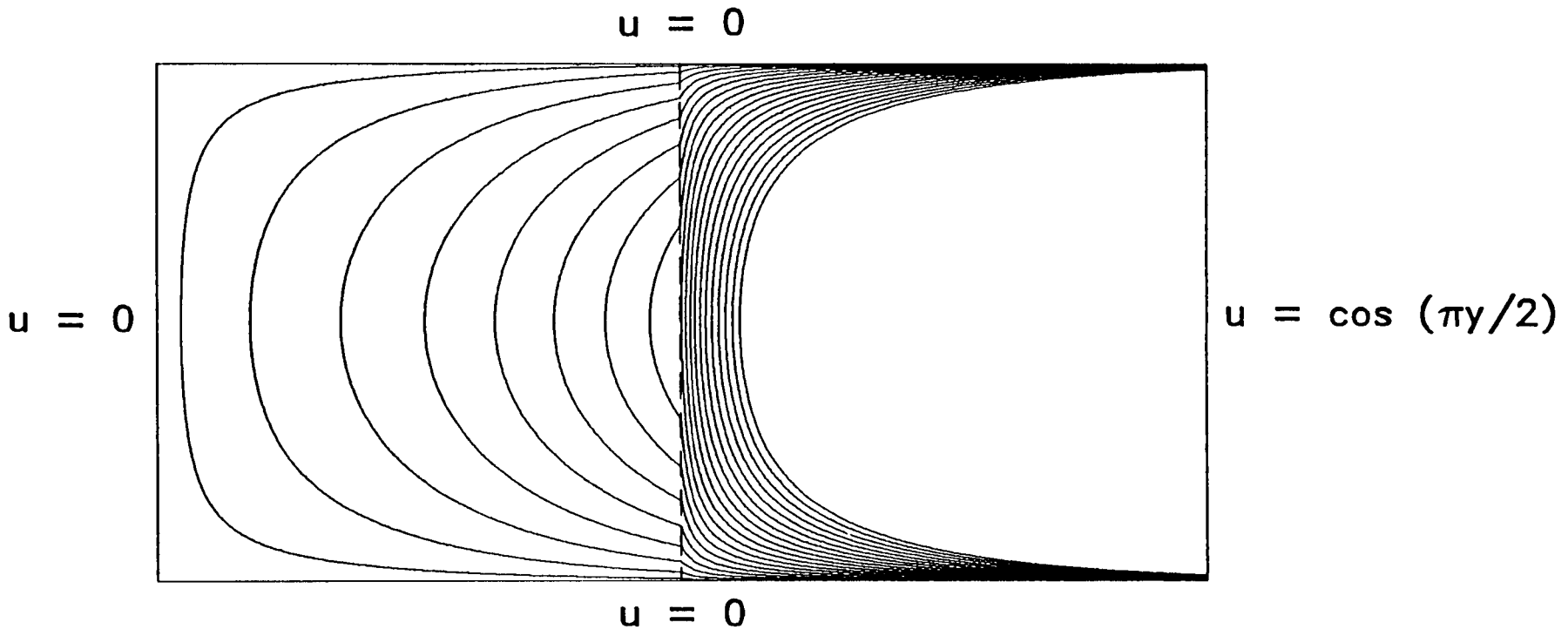

Figure 9. - Computed solution to equation (4); interface at dotted line.

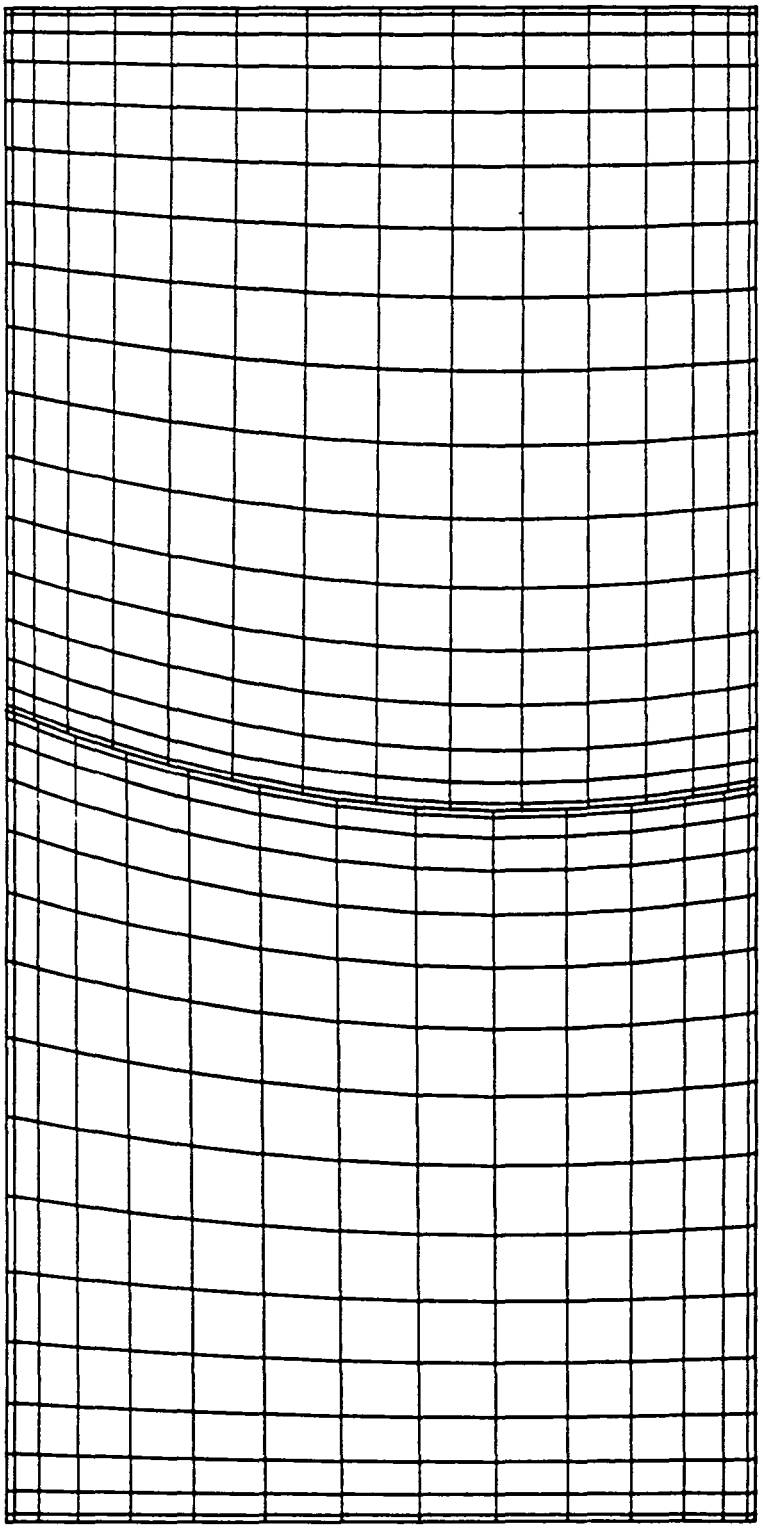

Figure 10. - Skewed two-domain mesh.

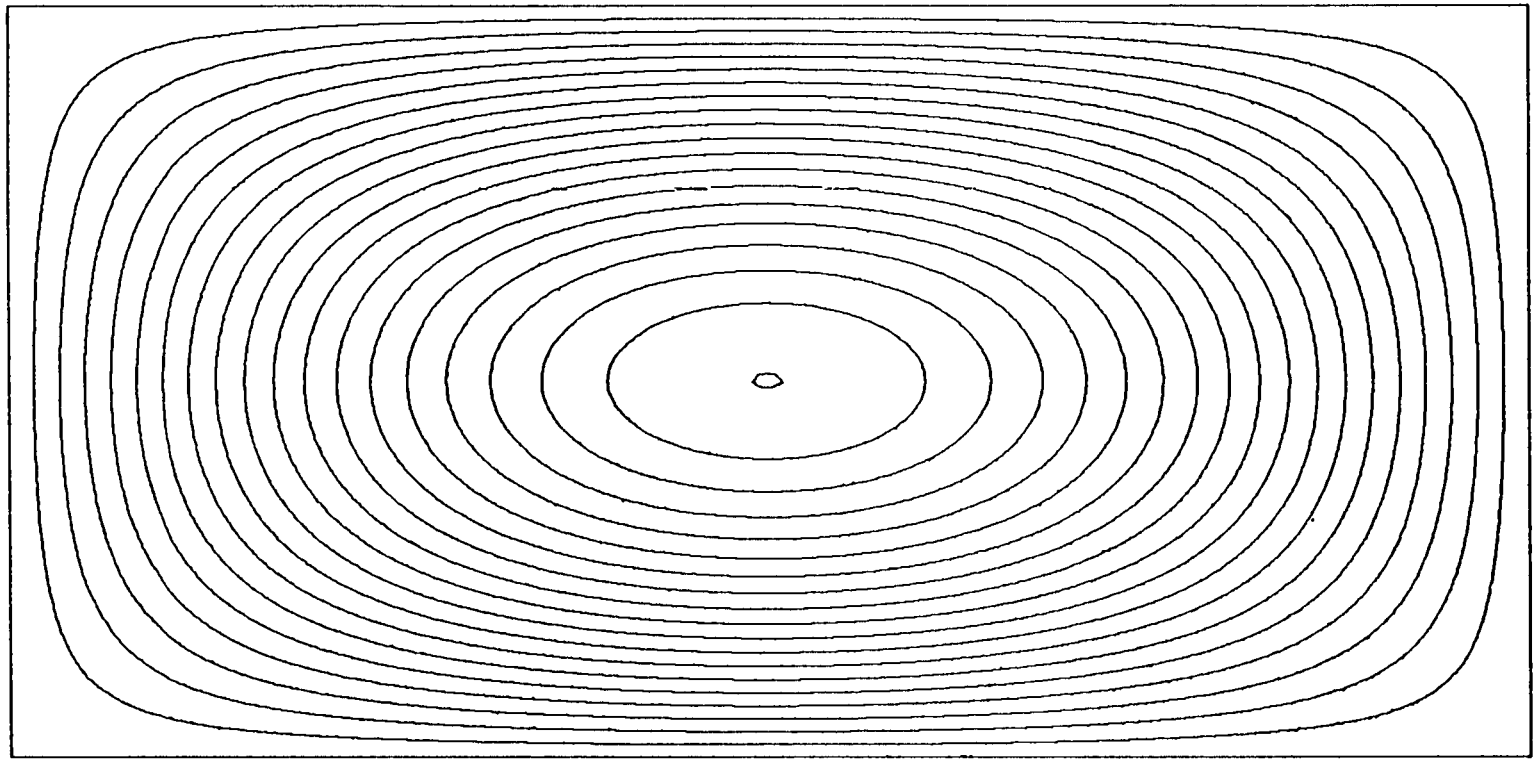

Figure 11. - Solution of equation (6) on mesh shown in fig. 10.

1 Report No NASA TM-87701	2 Government Accession No	3 Recipient's Catalog No
4 Title and Subtitle "A Spectral Multi-Domain Technique With Application To Generalized Curvilinear Coordinates"		5 Report Date March 1986
		6 Performing Organization Code 506-43-31-03
7 Author(s) Michèle G. Macaraeg & Craig L. Streett		8 Performing Organization Report No
9 Performing Organization Name and Address Langley Research Center Hampton, Virginia 23665-5225		10 Work Unit No
		11 Contract or Grant No
12 Sponsoring Agency Name and Address National Aeronautics and Space Administration Washington, DC 20546-0001		13 Type of Report and Period Covered Technical Memorandum
		14 Sponsoring Agency Code

15 Supplementary Notes

Presented at Antibes, France "Finite Element Methods in Flow Problems" The Sixth International Conference

Conference in Antibes, France June 16-20, 1986

16 Abstract

Spectral collocation methods have proven to be efficient discretization schemes for many aerodynamic (see e.g., refs. 1-5) and fluid mechanic (e.g., refs. 6-9) problems. The high-order accuracy and resolution shown by these methods allows one to obtain engineering-accuracy solutions on coarse meshes, or alternatively, to obtain solutions with very small error. One drawback to these techniques has been the requirement that a complicated physical domain must map into a simple computational domain for discretization. This mapping must be smooth if the high-order accuracy and expontential convergence rates associated with spectral methods are to be preserved (ref. 2). Additionally even smooth stretching transformations can decrease the accuracy of a spectral method, if the stretching is severe (ref. 5). A further difficulty with spectral methods has been in their implementation on parallel processing computers, where efficient spectral algorithms have been lacking.

The above restrictions are overcome in the present method by splitting the domain into regions, each of which preserve the advantages of spectral collocation, and allow the ratio of the mesh spacings between regions to be several orders of magnitude higher than allowable in a single domain. Such stretchings would be required to resolve the thin viscous region in an external aerodynamic problem. Adjoining regions are interfaced by enforcing a global flux balance which preserves high-order continuity of the solution, regardless of the type (diffusion- or advection-dominated) of the equations being solved.

17 Key Words (Suggested by Authors(s))	18 Distribution Statement
Spectral Methods Patched Grids Curvilinear Coordinates	Unclassified - Unlimited Subject Category-34

19 Security Classif (of this report)	20 Security Classif (of this page)	21 No. of Pages	22 Price
Unclassified	Unclassified	20	A02

For sale by the National Technical Information Service, Springfield, Virginia 22161 NASA-Langley, 1986

End of Document